N is required to model the transmission for a given accuracy. The larger N is, the less the error due to discretisation is when reconstructing the output signal. A finite number N causes an oscillation around the actual voltage value. An increase in N will augment the frequency and decrease the amplitude of the oscillation.[5] For a typical line of 100 mm length, $N = 20$ is a suitable compromise to achieve good accuracy and a reasonably small computing time.

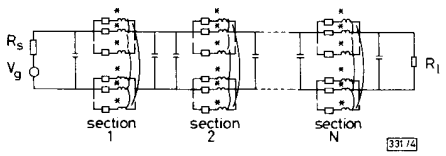

Fig. 4 *Equivalent circuit of dissipative interconnection used for SPICE simulations*

Typical time responses at the receiver end to a step input are shown in Fig. 5 for various line lengths l_0 (10 mm and 100 mm) and terminal loads ($R_l = 72\,\Omega$ and $R_l = 10\,k\Omega$). A step input signal of amplitude 1 V and of rise time 200 ps was applied. The driving load is $R_s = 72\,\Omega$ and equals in our case the characteristic impedance R_0 of the line.

The propagation delay of the output signal is 62 ps for $l_0 =$ 10 mm (Fig. 5*a*) and 620 ps for $l_0 = 100$ mm (Fig. 5*b*). The distortion of the output signal at the two ends of the step can be explained by the presence of higher harmonic components in the spectrum of the input signal which are more severely degraded by skin effect. The degradation of the rise time and of the waveform are rather high due to the line resistance for the longer line ($l_0 = 100$ mm) and are negligible for the shorter line ($l_0 = 10$ mm). Oscillations in the response due to the finite number of quadripoles N are much more important for the longer line.

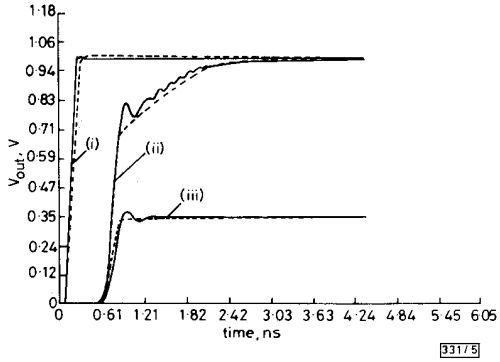

Fig. 5 *Time domain responses at line receiver end, with rise time of 200 ps*

(i) line length = 10 mm, $R_s = 72\,\Omega$, $R_l = 10\,k\Omega$ (open circuit)
(ii) line length = 100 mm, $R_s = 72\,\Omega$, $R_l = 10\,k\Omega$ (open circuit)
(iii) line length = 100 mm, $R_s = 72\,\Omega$, $R_l = 72\,\Omega$
– – – – simulation responses with FFT method[6]

In Fig. 5*c*, the loading conditions at the two ends of the 100 mm long line are $R_l = R_s = R_0 = 72\,\Omega$. The output voltage is only 0·36 V (attenuation due to the total line resistance of 54 Ω) and the oscillations are greatly reduced. This is because the adapted load decreases the reflections at the receiver end, and therefore each input impedance of every quadripole approaches the characteristic impedance of the line. As shown in Fig. 5, all these results are in good agreement with those obtained from in-house software.[6]

Moreover, the influence of the rise time T_r on the output signal has been analysed. It can be shown that the oscillatory behaviour is amplified and the waveform is more degraded when decreasing the rise time. This can be explained by an oscillatory amplitude increasing with $1/T_r$[5] and by higher harmonic components in the spectrum of the input signal.

Conclusion: Skin effect has been analysed in a microstrip from DC up to 10 GHz with a SPICE simulator (commonly used for nonlossy lines). Losses in the ground plane have properly been accounted for. Results obtained with our approach are in good agreement with other published data especially with those obtained by the FFT method. The influences of the rise time, of the load conditions and of the line length have been investigated. Our typical results show that the degradations due to the skin effect and the proximity effect losses are amplified when the rise time is shortened (in high speed logic circuits), when the load conditions are incorrectly adapted (nonlinear loads in logic circuits) and of course when the propagation line length is increased.

T. VU DINH
B. CABON
J. CHILO

Lemo BP257, 38016 Grenoble Cedex, France

8th October 1990

References

1 VU DINH, T., CABON, B., and CHILO, J.: 'New skin effect equivalent circuit', *Electron. Lett.*, 1990, **26**, (19), pp. 1582–1584
2 JOHNSON, R. R.: 'Multichip modules: next generation packages', *IEEE Spectrum*, March 1990, pp. 34–48
3 RUEHLI, A. E.: 'Inductance calculations in a complex integrated circuits environment', *IBM J. Res. Dev.*, 1972, pp. 470–480
4 WEI, C., HARRINGTON, R. F., MAUTZ, J. R., and SARKAR, T. R.: 'Multiconductor transmission lines in multilayers dielectric media', *IEEE Trans. MTT*, April 1984, **32**, pp. 439–450
5 BOSE, S., and BHATTACHARYYA, B. K.: 'Time domain method for optimizing transmission line model'. IEPS 8th International Electronics Packaging Conference, Dallas, 1988, pp. 637–664
6 CHILO, J., MONLLOR, C., and BOUTHINON, M.: 'Interconnection effects in fast logic integrated GaAs circuit', *Int. J. Elec.*, 1985, **58**, pp. 324–339

HIGH-FREQUENCY OUTPUT CHARACTERISTICS OF AlGaAs/GaAs HETEROJUNCTION BIPOLAR TRANSISTORS

Indexing terms: Bipolar devices, Transistors

A model has been developed which generates the high-frequency $i_c - v_{ce}$ output characteristics of bipolar transistors from computed cutoff frequency against current density data. The presented results, which can be used directly for large-signal modelling, are the first report of high-frequency output characteristics of bipolar transistors.

Although the bipolar transistor has been actively investigated in recent years, characterisation of this device has primarily been limited to reports of DC current–voltage behaviour, and network parameters (e.g. S_{11}, S_{12}, S_{21}, S_{22}), from which high-frequency-limited parameters (e.g. f_T, f_{max}) are calculated and small-signal equivalent circuits are derived at specified frequencies.[1–3] However, because these individual parameters are valid only at specified operating conditions (current, voltage, and junction temperature), these parameters are generally insufficient for the design of large-signal microwave circuits such as power amplifiers. Instead, the design of microwave circuits requires knowledge of the dynamic range of a transistor and its temperature dependence at given frequencies.

In this letter, we present the first calculation of high frequency output characteristics of a bipolar transistor that can be used directly in large-signal modelling. These output characteristics can be employed to determine the power efficiency of bipolar transistors under different bias conditions and loads for any specified operating frequency. Optimum load design for maximum efficiency can therefore be accomplished. Additionally, the output characteristics can be used to determine the exact output current and voltage waveforms for given

input waveforms, under specific bias and load conditions. Thus harmonic distortion of bipolar transistor amplifiers can be evaluated, and circuit parameters can be optimised. By modelling different transistor structures, these output characteristics can also be used for the design of individual devices.

In these calculations of the high frequency large-signal output characteristics, the electric properties of the transistor (such as depletion widths and velocity-field relations) are assumed to change instantaneously with the input RF signal. The temperature of the device, however, is expected to remain constant over the cycle of the output waveform. The first consideration is therefore determining the junction temperature resulting from the power dissipated in the transistor for the specified DC bias condition and RF signal. Assuming a perfectly linear transfer function and resistive load, for a voltage $v_{ce} = V_C + v_{cm} \cos \omega t$ and collector current $i_c = I_C - i_{cm} \cos \omega t$, the power dissipated in the bipolar transistor for class A, B and C amplification are given respectively by

$$P_d^A = I_C V_C - \frac{i_{cm} v_{cm}}{2} \tag{1}$$

$$P_d^B = \frac{i_{cm} V_C}{\pi} - \frac{i_{cm} v_{cm}}{4} \qquad (I_C = 0)$$

$$P_d^C = \frac{i_{cm} V_C}{\pi} \frac{\sin\theta - \theta\cos\theta}{1 - \cos\theta} - \frac{i_{cm} v_{cm}}{2\pi} \times \frac{\theta - \sin\theta\cos\theta}{1 - \cos\theta} \qquad \left(I_C = i_{cm} \frac{\cos\theta}{1 - \cos\theta}\right)$$

where 2θ $(0 < \theta < (\pi/2))$ is the conduction angle. The thermal resistance of the semiconductor is given by[4]

$$R_{th} = \frac{1}{2\kappa \cdot (l - w)} \cdot \ln\left[\frac{l(w + 2W_s)}{w(l + 2W_s)}\right] \tag{2}$$

where l, w are the length and width of the thermal source, W_s is the thickness of the substrate, and κ is the temperature-dependent thermal conductivity of the semiconductor. The junction temperature therefore follows from the product of the thermal resistance and dissipated power:

$$T_j = T_C + (R_C + R_{th}) \cdot P_d \tag{3}$$

where T_C $(= 300\,\text{K})$ is the case temperature. The package resistance $R_C (\ll R_{th})$ is neglected for appropriate heat sinking.

Using the constant junction temperature specified by the bias and driving signal, the cutoff frequency against collector current density j_c characteristic of the bipolar transistor can be calculated for various voltage bias conditions.[5] As usual, the unity current gain frequency is modelled by

$$f_T = \frac{1}{2\pi\tau_{ec}} \tag{4}$$

where the emitter-to-collector transit time is given by the emitter charging time, the base transit time, the current-induced-base transit time, the space-charge-layer delay time, and the collector charging time

$$\tau_{ec} = \tau_e + \tau_b + \tau_{CIB} + \tau_{SCL} + \tau_c \tag{5}$$

From this relation, the effective widening of the base at high current densities (Kirk effect) results in a falloff in f_T as the slow diffusion of carriers produces a significant τ_{CIB} contribution to the total emitter-to-collector transit time.[6]

From the $f_T - j_c$ characteristics, common-emitter current gains are computed at specified operating frequencies. The frequency dependence of common-emitter current gain is generally expressed by[7]

$$\beta(f) = \frac{\beta_0}{1 + j(f/f_\beta)} \tag{6}$$

where β_0 is the low-frequency current gain and f_β is the frequency at which the current gain drops to $\beta_0/\sqrt{(2)}$. At high frequencies $(f \gg f_\beta)$, eqn. 3 reduces to $|\beta| = \beta_0(f_\beta/f)$, and the definition of cutoff frequency f_T as the frequency at which $\beta = 1$, gives $f_T = \beta_0 f_\beta$. Therefore, at any specified operating frequency $f_0 (\gg f_\beta)$, the current gain can be defined by $\beta = f_T/f_0$. Applying the computed current gains to specified base currents i_b, the collector currents can be successively summed to produce i_c against v_{cb} curves. Adding the base–emitter bias v_{be} to v_{cb}, the total bias across the transistor junctions is then determined for each corresponding i_b, i_c data. Finally, by including the voltage drop across the emitter and collector series resistances (also specific to the particular bias condition), the total bias v_{ce} across the transistor is determined for corresponding i_b, i_c data, giving the high-frequency $i_c - v_{ce}$ output characteristics.

The model developed above was used to compute the high-frequency performance of an AlGaAs/GaAs heterojunction bipolar transistor (HBT) at junction temperatures specified by particular DC bias conditions and RF signals. For the current simulation, the basic epitaxial structure and device dimensions of the HBT investigated by Chang *et al.*[8] were adopted; these device parameters are listed in Table 1.

Table 1 HBT DEVICE PARAMETERS

Emitter area	$1{\cdot}2 \times 9{\cdot}0\,\mu\text{m}^2$
Base–emitter contact spacing	$0{\cdot}25\,\mu\text{m}$
Base contact width	$1{\cdot}0\,\mu\text{m}$
Collector–base contact spacing	$2{\cdot}5\,\mu\text{m}$
Collector area	$3{\cdot}3 \times 10{\cdot}0\,\mu\text{m}^2$
Thickness	**Dopant level**
Emitter $0{\cdot}2\,\mu\text{m}$	$5 \times 10^{17}\,\text{cm}^{-3}$
Base $0{\cdot}06\,\mu\text{m}$	$1 \times 10^{20}\,\text{cm}^{-3}$
Collector $0{\cdot}7\,\mu\text{m}$	$5 \times 10^{16}\,\text{cm}^{-3}$
Subcollector $0{\cdot}3\,\mu\text{m}$	$4 \times 10^{18}\,\text{cm}^{-3}$
Substrate $200\,\mu\text{m}$	

For the particular results simulated here, we first specified class A operation with a quiescent point at $V_C = 5\,\text{V}$, $I_C = 5\,\text{mA}$ and maximum RF signal amplitudes $v_{cm} = 4\,\text{V}$, $i_{cm} = 5\,\text{mA}$. For the resultant power dissipation of 15 mW and a calculated thermal resistance of 2·92 K/mW, an HBT operating temperature of 344 K is determined. Using this constant junction temperature, $f_T - j_c$ characteristics were simulated. Calculated curves for selected collector–base bias values are shown in Fig. 1. (The $f_T - j_c$ behaviour, and specifically the falloff in cutoff frequency due to high current effects was discussed in Reference 5.) Selecting an operating frequency of 10 GHz, we then computed the current gains, which were in turn used to generate the high-frequency $i_c - v_{ce}$ output characteristics. Shown in Fig. 2 is the output characteristic $i_b = 0{\cdot}5$ to 5·0 mA, of the AlGaAs/GaAs HBT described in Table 1, at a junction temperature of 344 K and an operating frequency

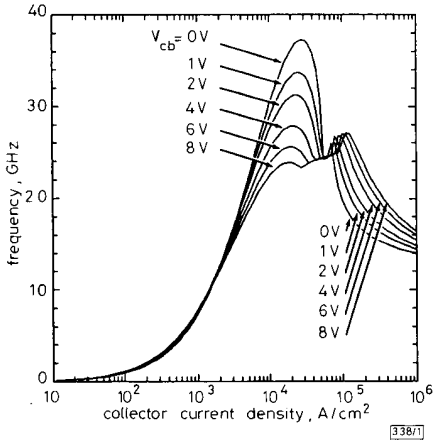

Fig. 1 *Unity current gain frequency f_T against collector current density j_c simulated at $T_j = 344$ K for selected collector–base bias V_{cb}*

of 10 GHz. These results, which can be used directly for both small-signal and large-signal design of HBT amplifier circuits, are the first report of high frequency output characteristics of a bipolar transistor.

Although the $i_c - v_{ce}$ characteristic of Fig. 2 exactly describes the HBT of Table 1 at the constant junction temperature of 344 K, because T_j was originally specified by a preselected bias and output waveform, in using these curves for large-scale modelling, some discrepancy with the transistor's actual operating temperature is introduced for the different input signals applied. Regardless of this possible discrepancy, however, these first-order $i_c - v_{ce}$ curves represent a useful tool for the design of HBT amplifiers. Additionally, this discrepancy is negligibly small for the nearly linear (i.e. low distortion) case. For a most precise analysis, these first-order curves can be used to analyse the large-signal operation of the device to yield a more accurate temperature, which can then be used to derive more exact output characteristics.

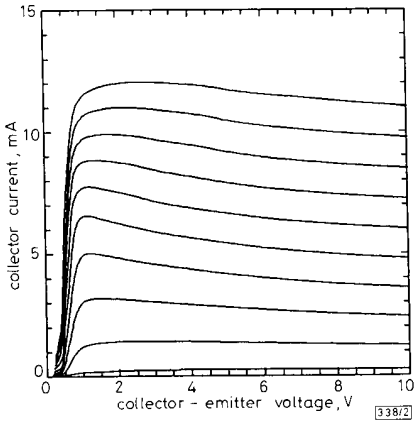

Fig. 2 *$i_c - v_{ce}$ output characteristics for HBT with parameters listed in Table 1, at operating frequency 10 GHz and constant junction temperature 344 K*

The junction temperature was selected for class A operation of the HBT at $V_C = 5$ V, $I_C = 5$ mA, $v_{cm} = 4$ V, $i_{cm} = 5$ mA
The base currents are swept from 0·5 to 5·0 mA in 0·5 mA steps

We have developed a model for characterising the high-frequency performance of HBTs. Using our model to calculate $f_T - j_c$ data, we derived high-frequency $i_c - v_{ce}$ output characteristics of the HBT. The presented $I - V$ curves for an AlGaAs/GaAs HBT at an operating frequency of 10 GHz is the first report of high-frequency output characteristics of a bipolar transistor. These characteristics can be directly used for the design of HBT amplifier circuits.

Acknowledgments: This work is supported by the Air Force Office of Scientific Research under contract no. AFOSR-89-0239 and the National Science Foundation under contract no. ECS-88-22406.

J. CHEN
G. B. GAO
M. S. ÜNLÜ
H. MORKOÇ

Coordinated Science Laboratory and Materials Research Laboratory
University of Illinois at Urbana-Champaign
1101 W. Springfield Avenue, Urbana, IL 61801, USA

G. B. Gao is on leave from Beijing Polytechnic University, Reliability Physics Laboratory, Beijing, China

8th October 1990

References

1 ASBECK, P. M., CHANG, M. F., WANG, K.-C., MILLER, D. L., SULLIVAN, G. J., SHENG, N. H., SOVERO, E., and HIGGINS, J. A.: 'Heterojunction bipolar transistors for microwave and millimeter-wave integrated circuits', *IEEE Trans.*, 1987, **ED-34**, pp. 2571–2579

2 BAYRAKTAROGLU, B., CAMILLERI, N., and LAMBERT, S. A.: 'Microwave performances of n-p-n and p-n-p AlGaAs/GaAs heterojunction bipolar transistors', *IEEE Trans.*, 1988, **MTT-36**, pp. 1869–1873

3 KIM, M. E., OKI, A. K., GORMAN, G. M., UMEMOTO, D. K., and CAMOU, J. B.: 'GaAs heterojunction bipolar transistor device and IC technology for high-performance analog and microwave applications', *IEEE Trans.*, 1989, **MTT-37**, pp. 1286–1303

4 GAO, G. B., ÜNLÜ, M. S., MORKOÇ, H., and BLACKBURN, D. L.: 'Emitter ballasting resistance design for, and current handling capability of AlGaAs/GaAs power heterojunction bipolar transistors', *IEEE Trans. Electron Devices* (in press)

5 CHEN, J., GAO, G. B., and MORKOÇ, H.: 'The thermal dependence of HBT high-frequency performance', *Electron. Lett.*, 1990, **26**, (21), pp. 1770–1772

6 GAO, G. B., ROULSTON, D. J., and MORKOÇ, H.: 'Design study of AlGaAs/GaAs HBT's', *IEEE Trans.*, 1990, **ED-37**, pp. 1199–1208

7 PRITCHARD, R. L.: 'Electrical characteristics of transistors' (McGraw-Hill, New York, 1967), p. 342

8 CHANG, M. F., ASBECK, P. M., WANG, K. C., SULLIVAN, G. J., SHENG, N., HIGGINS, J. A., and MILLER, D. L.: 'AlGaAs/GaAs heterojunction bipolar transistors fabricated using a self-aligned dual-lift-off process', *IEEE Electron Device Lett.*, 1987, **EDL-8**, pp. 303–305

ACCURATE REFLECTANCE AND OPTICAL FIBRE BACKSCATTER PARAMETER MEASUREMENTS USING AN OTDR

Indexing term: Optical fibres

A method for accurate reflectance measurement is described. The technique introduces a variable attenuator in a recirculating loop to calibrate the reflection provided by a fictitious reflector. A formula for this calibrated reflection is given. The device allows accurate measurements of the backscatter parameter of a fibre.

Introduction: For reflectance measurements, various techniques or devices are usually proposed as reference elements; bare fibre endface giving Fresnel reflection, cleaved or polished fibre-end dipped in oils having known refractive index, or fibre endface mirrored by metal or dielectric multilayers. All these techniques which are based upon fibre endface reflection give rise to several problems such as tilting of the fibre-end,[1] defects in endface quality[2] or true refractive index (of fibre core or oils) determination. Such imperfections lead to uncertainty about the true reflectance value and are inconsistent with the requirements of an absolute reference. That is why we have developed a method of calibration which, with our previous work on reflection coefficient modelling,[3] gives a reflection standard.

Reflectance formula: The reflectance R (dB) corresponding to a reflective element can be written as[3]

$$R\,(\mathrm{dB}) = 10 \log_{10}\{K \,.\, E_R/P_s\} \tag{1}$$

where E_R is the reflected pulse energy, and P_s is the backscattered power value at the reflective element abscissa. K (with the dimensions of frequency) is obtained from the optical fibre parameters. If K is known, one can determine any reflectance in the link from the measured values of the reflected pulse energy E_R and the backscattered power P_s.

Optical fibre characteristics determination: To achieve accurate measurement of the reflectance R, the value of the parameter K must be precisely determined. The K value can be derived from the formula

$$K = 0{\cdot}5\alpha(z)S(z)V_g \tag{2}$$

by using known values of the pulse group velocity V_g, the scattering coefficient $\alpha_s(z)$ and the backscattering factor $S(z)$. A precise K-value calibration is supposed to take into account the actual fibre imperfection contribution instead of considering a perfect fibre. This value can be reached accurately